

commands into control signals for the motors, the electric circuit that delivers power to the motors, and the gearbox and tracks that propel the tank. The tank has two tracks, left and right, each driven by its own brushless direct-current (DC) motor. A gearbox connects each motor to the sprocket wheel of its track. The operator drives the tank by setting the duty ratio of the voltage signal at the terminals of the motors. The duty ratio are set using the control sticks on a gamepad and sent via a wireless network to the computer.

The computer generates two periodic voltage signals, one for each motor. The motor's duty ratio is the fraction of time that it is turned on in one period of the signal (i.e., its ON time). Because the battery voltage is fixed, the power delivered to a motor is proportional to its duty ratio. Driving the tank is straightforward. If the duty ratio of the left and right motors are equal then the tank moves in a straight line. The tank spins clockwise if the duty ratio of the left motor is higher than that of the right motor. The tank spins counterclockwise if the duty ratio of the right motor is higher than that of the left motor. A high duty ratio causes the tank to move quickly; a low duty ratio causes the tank to move slowly.

If the voltage signal has a high frequency, then the inertia of the motor will carry it smoothly through moments when it is disconnected from the batteries; the motors operate efficiently and the tank handles well. If the frequency is too low, then the motor operates inefficiently. It speeds up when the batteries are connected, slows down when they are disconnected, and speeds up again when power is reapplied. This creates heat and noise, wasting energy and draining the batteries without doing useful work. Therefore, we want the voltage signal to have a high frequency.

Unfortunately, a high-frequency signal means less time for the computer to process data from the radio. If the frequency is too high, then there is a noticeable delay as the tank processes commands from the operator. At some point, the computer will be completely occupied with the motors, and when this happens, the tank becomes unresponsive.

Somewhere in between is a frequency that is both acceptable to the driver and efficient enough to give a satisfactory battery life. There are physical limits on the range of usable frequencies. It cannot be so high that the computer is consumed entirely by the task of driving the motors. It cannot be so low that the tank lurches uncontrollably or overheats its motors and control circuits. Within this range, the choice of frequency depends on how sensitive the driver is to the nuances of the tank's control.

An acceptable frequency could be selected by experimenting with the real tank; let a few people drive it around using different frequencies and see which they like best. If we use the real tank to do this, then we can get the opinions of a small number of people about a small number of frequencies. The tank's batteries are one constraint on the number of experiments that can be conducted. They will run dry after a few trials and need several hours to recharge. That we have only one tank is another constraint. Experiments must be conducted one at a time. If, however, we build a simulation of the tank, then we can give the simulator to anyone who cares to render an opinion, and that person can try as many different frequencies as time and patience permit.

**TABLE 2.1** Value of Parameters Used in the Tank's Equations of Motion

Parameter	Value	Description
$m_t$	0.8 kg	Mass of the tank
$J_t$	$5 \times 10^{-4} \text{ kg} \cdot \text{m}^2$	Angular mass of the tank
$B$	0.1 m	Width of the tank from track to track
$B_r$	$1.0 \text{ N} \cdot \text{s} / \text{m}$	Mechanical resistance of the tracks to rolling forward
$B_s$	$14.0 \text{ N} \cdot \text{s} / \text{m}$	Mechanical resistance of the tracks to sliding forward
$B_l$	$0.7 \text{ N} \cdot \text{m} \cdot \text{s} / \text{rad}$	Mechanical resistance of the tracks to turning
$S_l$	$0.3 \text{ N} \cdot \text{m}$	Lateral friction of the tracks

### 2.2.1 Equations of Motion

The model of the tank's motion is adapted from Anh Tuan Le's PhD dissertation [74]. The model's parameters are listed in Table 2.1, and the coordinate system and forces acting on the tank are illustrated in Figure 2.2. The model assumes that the tank is driven on a hard, flat surface and that the tracks do not slip. The position of the tank is given by its  $x$  and  $y$  coordinates. The heading  $\theta$  of the tank is measured with respect to the  $x$  axis of the coordinate system and the tank moves in this direction with a speed  $v$ .

The left track pushes the tank forward with a force  $F_l$ ; the right track, with a force  $F_r$ ; and  $B_r$  is the mechanical resistance of the tracks to rolling. The tank uses skid steering; to turn, the motors must collectively create enough torque to cause the tracks to slide sideways. This requires overcoming the sticking force  $S_l$ . When sufficient torque is created, the vehicle begins to turn. As it turns, some of the propulsive force is expended to drag the tracks laterally; this is modeled by an additional resistance  $B_l$  to its turning motion and  $B_s$  to its rolling motion.

The tank's motion is described by two sets of equations, one for when the tank is turning and one for when it is not. The switch from turning to not turning (and vice

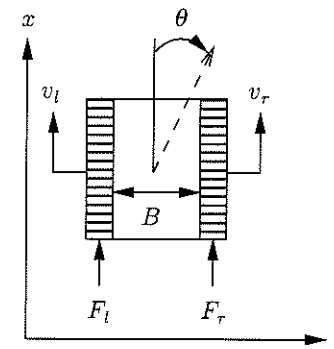


**FIGURE 2.2** Coordinate system, variables, and parameters used in the tank's equations of motion.

versa) has two discrete effects: (1) the angular velocity  $\omega$  changes instantaneously to and remains at zero when the tracks stick and the turn ends, and (2) the rolling resistance of the tank changes instantaneously when the tank starts and ends a turn. The Boolean variable *turning* is used to change the set of equations. The equations that model the motion of the tank are

$$\text{turning} = \begin{cases} \text{true} & \text{if } \frac{B}{2}|F_l - F_r| \geq S_l \\ \text{false} & \text{otherwise} \end{cases} \quad (2.1)$$

$$\dot{v} = \begin{cases} \frac{1}{m_t}(F_l + F_r - (B_r + B_s)v) & \text{if } \text{turning} = \text{true} \\ \frac{1}{m_t}(F_l + F_r - B_r v) & \text{if } \text{turning} = \text{false} \end{cases} \quad (2.2)$$

$$\dot{\omega} = \begin{cases} \frac{1}{J_t}\left(\frac{B}{2}(F_l - F_r) - B_l \omega\right) & \text{if } \text{turning} = \text{true} \\ 0 & \text{if } \text{turning} = \text{false} \end{cases} \quad (2.3)$$

$$\dot{\theta} = \omega \quad (2.4)$$

$$\dot{x} = v \sin(\theta) \quad (2.5)$$

$$\dot{y} = v \cos(\theta) \quad (2.6)$$

$$\text{If } \text{turning} = \text{false then } \omega = 0 \quad (2.7)$$

When *turning* changes from false to true, every state variable evolves from its value immediately prior to starting the turn, but using the equations designated for *turning* = true. When *turning* changes from true to false, every state variable except  $\omega$  evolves from its value immediately prior to ending the turn, but using the equations designated for *turning* = false;  $\omega$  changes instantaneously to zero and remains zero until the tank begins to turn again.

These differential equations describe how the tank moves in response to the propulsive force of the tracks. The track forces  $F_l$  and  $F_r$  are inputs to this model, and we can take any function of the state variables— $v$ ,  $\omega$ ,  $\theta$ ,  $x$ , and  $y$ —as output. For reasons that will soon become clear, we will use the speed with respect to the ground of the left and right treads; Figure 2.2 illustrates the desired quantities. The speed  $v_l$  of the left tread and speed  $v_r$  of the right tread are determined from the tank's linear speed  $v$  and rotational speed  $\omega$  by

$$v_l = v + B\omega/2 \quad (2.8)$$

$$v_r = v - B\omega/2 \quad (2.9)$$

The dependence of the input on the output is denoted by the function

$$\begin{bmatrix} v_l(t) \\ v_r(t) \end{bmatrix} = M \left( [F_l(t) \ F_r(t)]^T \right) \quad (2.10)$$

This function accepts the left and right tread forces as input and produces the left and right tread speeds as output.

How were the values in Table 2.1 obtained? Two of them were measure directly: the mass of the tank with a postal scale and the width of the tank with a ruler. The angular mass of the tank is an educated guess. Given the width  $w$  and length  $l$  of the tank's hull, which were measured with a ruler, and the mass, obtained with a postal scale, the angular mass is computed by assuming the tank is a uniformly dense box. With these data and assumptions, we have

$$J_t = \frac{m_t}{12}(w^2 + l^2)$$

This is not precise, but it is the best that can be obtained with a ruler and scale.

The resistance parameters are even more speculative. The turning torque  $S_l$  was computed from the weight  $W$  of the tank and length  $l_t$  of the track, which were both measured directly, a coefficient of static friction  $\mu_s$  for rubber from Serway's *Physics for Scientists and Engineers* [133], and the approximation

$$S_l = \frac{W l_t \mu_s}{3}$$

from Le's dissertation [74]. The resistances  $B_r$  and  $B_s$  to forward motion and resistance  $B_l$  to turning were selected to give the model reasonable linear and rotational speeds.

This mix of measurements, rough approximations, and educated guesses is not uncommon. It is easier to build a detailed model than to obtain data for it. The details, however, are not superfluous. The purpose of this model is to explore how the tank's response to the driver changes with the frequency of the power signal sent to the motors. For this purpose it is necessary to include those properties of the tank that determine its response to the intermittent voltage signal: specifically, inertia and friction.

## 2.2.2 Motors, Gearbox, and Tracks

The motors, gearbox, and tracks are an electromechanical system for which the method of bond graphs is used to construct a dynamic model (Karnopp et al. [61] give an excellent and comprehensive introduction to this method). The bond graph model is coupled to the equations of motion by using Equation 2.10 as a bond graph element. This element has two ports, one of which has the effort variable  $F_l$  and flow variable  $v_l$ , and the other, the effort variable  $F_r$  and flow variable  $v_r$ . The causality

of this element is determined by the functional form of Equation 2.10: it is supplied with the effort variables and produces the flow variables. This was the reason for selecting the track speeds as output.

The model of the motors, gearbox, and tracks accounts for the inductance and internal resistance of the electric motors, the angular mass and friction of the gears, and the compliance of the rubber tracks. The electric motors are Mabuchi FA-130 Motors, the same type of DC motor that is ubiquitous in small toys. One motor drives each track. The motors are plugged into a Tamiya twin-motor gearbox. This gearbox has two sets of identical, independent gears that turn the sprocket wheels. The sprocket wheels and tracks are from a Tamiya track-and-wheel set; the tracks stretch when the tank accelerates (in hard turns this causes the tracks to come off the wheels!), and so their compliance is included in the model.

To drive the motors, the computer switches a set of transistors in an Allegro A3953 full-bridge pulsewidth-modulated (PWM) motor driver. When the switches are closed, the tank's batteries are connected to the motors. When the switches are open, the batteries are disconnected from the motors. The transistors can switch on and off at a rate three orders of magnitude greater than the rate at which the computer can operate them, and power lost in the circuit is negligible in comparison to inefficiencies elsewhere in the system. The batteries and motor driver are, therefore, modeled as an ideal, time varying voltage source.

A sketch of the connected motors, gearbox, and tracks and its bond graph are shown in Figure 2.3. Table 2.2 lists the parameters used in this model. The differential

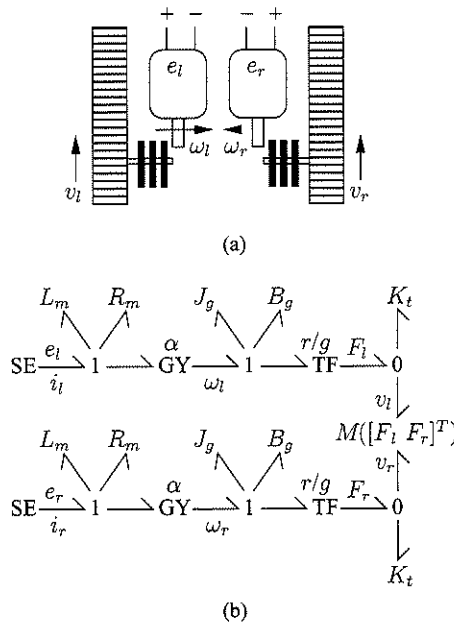


FIGURE 2.3 Motors, gears, and tracks of the tank: (a) diagram; (b) bond graph.

TABLE 2.2 Parameters of the Motors, Gearbox, and Tracks

Parameter	Value	Description
$L_m$	$10^{-3}$ H	Inductance of the motor
$R_m$	$3.1 \Omega$	Resistance of the motor
$J_g$	$1.2 \times 10^{-6}$ kg · m <sup>2</sup>	Angular mass of the gears
$B_g$	$6.7 \times 10^{-7}$ N · m · s / rad	Mechanical resistance of the gears to rotation
$g$	204	Gear ratio of the gearbox
$\alpha$	$10^{-3}$ N · m / A	Current-torque ratio of the electric motor
$r$	0.015 m	Radius of the sprocket wheel
$K_t$	$10^{-3}$ m / N	Compliance of the track

equations are read directly from the bond graph:

$$i_l = \frac{1}{L_m}(e_l - i_l R_m - \alpha \omega_l) \tag{2.11}$$

$$\omega_l = \frac{1}{J_g} \left( \alpha i_l - \omega_l B_g - \frac{r}{g} F_l \right) \tag{2.12}$$

$$\dot{F}_l = \frac{1}{K_t} \left( \frac{r}{g} \omega_l - v_l \right) \tag{2.13}$$

$$i_r = \frac{1}{L_m}(e_r - i_r R_m - \alpha \omega_r) \tag{2.14}$$

$$\omega_r = \frac{1}{J_g} \left( \alpha i_r - \omega_r B_g - \frac{r}{g} F_r \right) \tag{2.15}$$

$$\dot{F}_r = \frac{1}{K_t} \left( \frac{r}{g} \omega_r - v_r \right) \tag{2.16}$$

where  $e_l$  and  $e_r$  are the motor voltages and  $v_l$  and  $v_r$  are the track speeds given by Equations 2.8 and 2.9.

Values for the parameters in Table 2.2 were obtained from manufacturers' data, from measurements, and by educated guesses. The gear ratio  $g$  and current-torque ratio  $\alpha$  are provided by the manufacturers. The gear ratio is accurate and precise (especially with respect to the values of other parameters in the model). The current-torque ratio is an average of the two cases supplied by Mabuchi, the motor's manufacturer. The first case is the motor operating at peak efficiency, and the second case is the motor stalling. The difference between these two cases is small, suggesting that  $\alpha$  does not vary substantially as the load on the motor changes. The estimate of  $\alpha$  is, therefore, probably very reasonable.

The radius  $r$  of the sprocket wheel and the resistance  $R_m$  and inductance  $L_m$  of the motor were measured directly. A ruler was used to measure the radius of the sprocket wheel. To determine  $R_m$  and  $L_m$  required more effort. The current  $i$  through

The unloaded motor is related to the voltage  $e$  across the motor by the differential equation

$$\dot{i} = \frac{1}{L_m}(e - iR_m) \quad (2.17)$$

The parameters  $L_m$  and  $R_m$  were estimated by connecting a 1.5-V C battery to the motor and measuring, with an oscilloscope, the risetime and steady state of the current through the motor. Let  $i_f$  be the steady-state current,  $t_r$  the risetime, and  $0.9i_f$  the current at time  $t_r$  (i.e., the risetime is the amount of time to go from zero current to 90% of the steady-state current). At steady state  $\dot{i} = 0$  and the resistance of the motor is given by

$$R_m = \frac{e}{i_f}$$

The transient current is needed to find  $L_m$ . The transient current is given by the solution to Equation 2.17:

$$i(t) = \frac{e}{R_m} \left( 1 - \exp\left(-\frac{R_m}{L_m}t\right) \right) \quad (2.18)$$

Substituting  $0.9i_f$  for  $i(t)$  and  $t_r$  for  $t$  in Equation 2.18 and solving for  $L_m$  gives

$$\frac{1}{L_m} = -\frac{1}{R_mt_f} \ln\left(1 - 0.9\frac{R_m}{e}i_f\right) = -\frac{i_f}{et_f} \ln(0.1) \approx 2.3\frac{i_f}{et_f}$$

Equivalently

$$L_m \approx 0.652 \frac{t_f}{i_f}$$

A similar experiment was used to obtain  $B_g$ . In this experiment, the motor was connected to the gearbox. As before, an oscilloscope was used to measure the risetime and steady-state value of the current through the motor. The rotational velocity  $\dot{\omega}$  of the motor is given by

$$\dot{\omega} = \frac{1}{J_g}(\alpha i - \dot{\omega}B_g)$$

The manufacturer gives the speed of the motor when operating at peak efficiency as 731.6 radians per second (rad/s). At steady state  $\dot{\omega} = 0$ . The steady state current

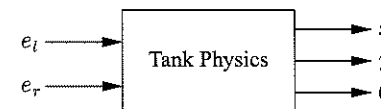


FIGURE 2.4 Input and output of the model of the tank's physics.

$i_f$  is measured with the oscilloscope. With  $i_f$  and the motor speed, the mechanical resistance of the gearbox is given by

$$B_g \approx \frac{\alpha i_f}{\dot{\omega}} = 1.37 \times 10^{-6} i_f$$

The angular mass  $J_g$  of the gearbox was estimated from its mass  $m_{gb}$ , radius of the gears  $r_{gb}$ , and the assumption that the mass is uniformly distributed in a cylinder. With this set of measurements and assumptions, the angular mass is

$$J_g = m_{gb}r_{gb}^2$$

The compliance of the tracks is an order-of-magnitude approximation. The tracks can be stretched by only a few millimeters before they slip off the wheels. The maximum propulsive force of the track is about a newton. The order of magnitude of the track compliance is, therefore, estimated to be  $10^{-3}$  meters/10<sup>0</sup> newtons, or about  $10^{-3}$  m/N.

### 2.2.3 Complete Model of the Tank's Continuous Dynamics

Equations 2.1–2.9 and 2.11–2.16 collectively describe the physical behavior of the tank. The equations of motion and the equations for the motors, gearbox, and tracks were developed separately, but algorithms for solving them work best when coupled equations are lumped together. Consequently, these are put into a single functional model called “tank physics,” which is illustrated in Figure 2.4. The inputs to the tank are the voltages across its left and right motors; these come from the computer. The output of the tank is its position and heading; these are observed by the tank's operator. The complete state space model of the tank's physical dynamics is

$$\text{turning} = \begin{cases} \text{true} & \text{if } \frac{B}{2}|F_l - F_r| \geq S_l \\ \text{false} & \text{otherwise} \end{cases} \quad (2.19)$$

$$\dot{v} = \begin{cases} \frac{1}{m_t}(F_l + F_r - (B_r + B_s)v) & \text{if turning} = \text{true} \\ \frac{1}{m_t}(F_l + F_r - B_r v) & \text{if turning} = \text{false} \end{cases} \quad (2.20)$$

$$\omega = \begin{cases} \frac{1}{J_t} \left( \frac{B}{2} (F_l - F_r) - B_l \omega \right) & \text{if } turning = \text{true} \\ 0 & \text{if } turning = \text{false} \end{cases} \quad (2.21)$$

$$\dot{\theta} = \omega \quad (2.22)$$

$$\dot{x} = v \sin(\theta) \quad (2.23)$$

$$\dot{y} = v \cos(\theta) \quad (2.24)$$

$$\text{If } turning = \text{false then } \omega = 0 \quad (2.25)$$

$$\dot{i}_l = \frac{1}{L_m} (e_l - i_l R_m - \alpha \omega_l) \quad (2.26)$$

$$\omega_l = \frac{1}{J_g} \left( \alpha i_l - \omega_l B_g - \frac{r}{g} F_l \right) \quad (2.27)$$

$$\dot{F}_l = \frac{1}{K_t} \left( \frac{r}{g} \omega_l - \left( v + \frac{B \omega}{2} \right) \right) \quad (2.28)$$

$$\dot{i}_r = \frac{1}{L_m} (e_r - i_r R_m - \alpha \omega_r) \quad (2.29)$$

$$\omega_r = \frac{1}{J_g} \left( \alpha i_r - \omega_r B_g - \frac{r}{g} F_r \right) \quad (2.30)$$

$$\dot{F}_r = \frac{1}{K_t} \left( \frac{r}{g} \omega_r - \left( v - \frac{B \omega}{2} \right) \right) \quad (2.31)$$

This model has 11 state variables— $v$ ,  $\omega$ ,  $\theta$ ,  $x$ ,  $y$ ,  $i_l$ ,  $\omega_l$ ,  $F_l$ ,  $i_r$ ,  $\omega_r$ , and  $F_r$ ; two input variables— $e_l$  and  $e_r$ ; and three output variables— $x$ ,  $y$ , and  $\theta$ .

## 2.2.4 The Computer

The computer, a TINI microcontroller from Maxim, receives commands from the operator through a wireless network and transforms them into voltage signals for the motors. The computer extracts raw bits from the Ethernet that connects the computer and the radio, puts the bits through the Ethernet and User Datagram Protocol (UDP) stacks to obtain a packet, obtains the control information from that packet, and stores that information in a register where the interrupt handler that generates voltage signals can find it. The interrupt handler runs periodically, and it has a higher priority than the thread that processes commands from the operator. Therefore, time spent in the interrupt handler is not available to process commands from the operator.

The frequency of the voltage signal is determined by the frequency of the interrupt handler. Frequent interrupts create a high-frequency voltage signal; infrequent interrupts, a low-frequency signal. Figure 2.5 illustrates how the interrupt handler works. It is executed every  $N$  machine cycles and at each invocation adds 32 to a counter stored in an 8-bit register. The counter is compared to an ON time that is set,

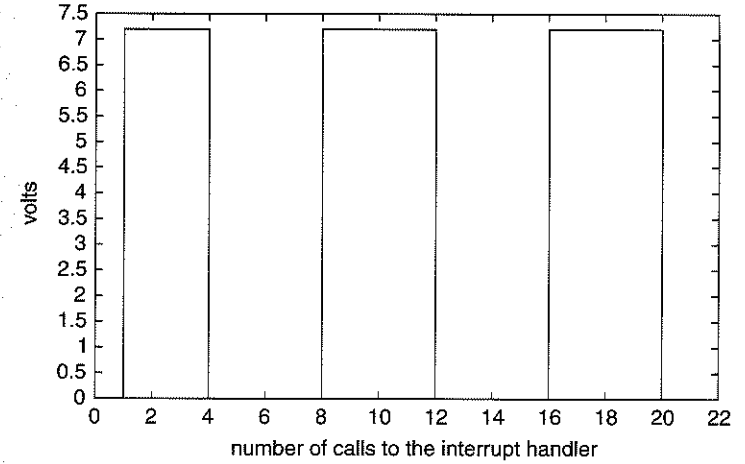


FIGURE 2.5 Generating a voltage signal with the interrupt handler.

albeit indirectly, by the operator. If the counter is greater than or equal to the ON time, then the motor is turned off. If the counter is less than the ON time, then the motor is turned on. If, for example, the tank is operating at full power, then the ON time for both motors is 255 and the motors are always on; if the motors are turned off, then the ON time is zero.

In Figure 2.5, the counter is initially zero and the motors are turned off. The ON time is 128. The first call to the interrupt handler adds 32 to the counter, compares  $32 < 128$ , and turns the motor on by connecting it to the tank's 7.2-V battery pack. At call 4, the counter is assigned a value of 128, which is equal to the ON time, and the motor is shut off. At call 8, the counter rolls over and the motor is turned on again.

The code in the interrupt handler is short; it has 41 assembly instructions that require 81 machine cycles to execute. According to the computer's manufacturer, there are  $18.75 \times 10^6$  machine cycles per second, which is one cycle every  $0.0533 \times 10^{-6}$  s ( $0.0533 \mu$ s). The interrupt handler, therefore, requires  $0.432 \times 10^{-6}$  s ( $0.432 \mu$ s) to execute. The frequency of the voltage signal is determined by how quickly the interrupt handler rolls the counter over. On average, eight calls to the interrupt handler complete one period of the voltage signal. The length of this period is  $8 \times (0.432 \times 10^{-6} + 0.0533 \times 10^{-6} \times N)$ . We can choose  $N$  and thereby select the period of the voltage signal; the frequency  $f_e$  due to this selection is

$$f_e \approx \frac{10^6}{3.46 + 0.426N} \quad (2.32)$$

The discrete-event model of the interrupt handler has two types of events: *Start interrupt* and *End interrupt*. The *Start interrupt* event sets the interrupt indicator to true and schedules an *End interrupt* to occur  $0.432 \times 10^{-6}$  s later. The *End interrupt* event increments the counter, sets the motor switches, sets the interrupt indicator to